ELSEVIER

Polymer 41 (2000) 5749–5757

polymer

Crystallisation of poly(3-hydroxybutyrate)/polyvinyl acetate blends

J.N. Hay*, L. Sharma

The School of Metallurgy and Materials, The University of Birmingham, Edgbaston, Birmingham B15 2TT, UK

Received 20 October 1998; received in revised form 1 September 1999; accepted 27 October 1999

Abstract

Poly(3-hydroxybutyrate) (PHB) has been blended with poly(vinyl acetate) (PVAc) and the system has been found to be miscible over the complete composition range studied, i.e. 0–100 wt%. The blends exhibited a single glass transition temperature, which varied with composition between the limits of the two homopolymers. Positive deviation from a linear dependence of the glass transition temperature with composition was observed and a molecular interaction parameter determined. At temperatures close to the melting point, the rates of bulk crystallisation as measured by DSC were found to increase with PVAc content. This was not observed in crystallising close to the glass transition temperature, where addition of PVAc not only increased the T_g but also retarded the crystallisation. Hot-stage microscopy confirmed that the spherulitic radial growth rates were reduced by the addition of PVAc, but this was not due to the lowering of the equilibrium melting point. This study also showed that the nucleation density was greater in the blends than in PHB itself. The anomalous increase in the bulk crystallisation rates has been attributed to an increase in the nucleation density produced in blending with PVAc. PHB is a bacteriological polymer and is low in impurities which can act as nuclei for crystallisation, such that few spherulites are observed in the light microscope. Blending with PVAc was considered to add impurities with a resulting increase in nucleation density in the blends.

Keywords: Poly(3-hydroxybutyrate); Polyvinyl acetate; Blends

1. Introduction

The commercially important biodegradable plastic, Biopol, is widely used in packaging [1,2] and in medical applications [3–11]. It is a copolymer of D-(−)-3-hydroxybutyrate with 8% of 3-D-(−)-hydroxyvalerate but since the natural product is highly stereospecific and the comonomer units are diastereoisomers [12], the copolymer is highly crystalline. The polymer undergoes an ageing process [13–16] on storage at room temperature, which renders it increasingly brittle and this has been attributed to the increase development of secondary crystallisation [15–18]. Storage at or above room temperature is accompanied by a logarithmic increase in crystallinity with time and a progressive production of a low-temperature melting endotherm some 30–50 K above the storage temperature. This has been attributed to the production of thin lamellae between the thicker lamellae which were produced during the initial stages of growth of the spherulites. These thinner lamellae help to reinforce the amorphous domains, stiffen the whole structure and produce embrittlement. The extent and rate of development of secondary crystallisation can be restricted by control of the crystalline morphology in particular by annealing or recrystallisation at elevated temperatures. This is attributed to preferential rejection of the valerate units by the crystalline units and the subsequent reduction in secondary crystallisation by the increased valerate concentration in the amorphous domains.

This approach has limited application since it requires annealing for extended periods at elevated temperatures. An alternative way of reducing the extent of ageing on storage is to increase the valerate content in the copolymer but this alters the material properties by too much [19]. Reducing the rates of crystallisation, by blending with a soluble homopolymer, is considered in this paper.

PHB blends have been examined by others [20]. These include polyethylene oxide [21,22], polysaccharides [23,24], polylactides [25] and poly(methyl methacrylate) [26,27]. The phase diagrams of the blends are complicated and, for example, both polyethylene oxide and PHB can crystallise as separate phases and the amorphous domains contain both miscible polymers with a variable composition depending on the extent to which they have crystallised and the initial composition.

The partial miscibility of PHB in PMMA has been extensively studied by Scandola et al. [26] and Yoon et al.

* Corresponding author. Tel.: +44-1214-144544; fax: +44-1214-145232.

0032-3861/00/$ - see front matter
PII: S0032-3861(99)00807-1

Table 1
Homopolymers and copolymer characteristics

Material	Properties	Additives
PHB—homopolymer	Melting point: 180°C Density: 1.22–1.25 g cm^{-3} Soluble in chloroform and methylene chloride $T_g = 0$°C $M_n = 131$ kg; $M_w = 539$ kg GPC using polystyrene as ref material	
XB111—copolymer	Melting point: 180°C $T_g = 5$°C	1% Boron nitride nucleating agent
PVAc	$T_g = 36$°C $M_n = 40$ kg; $M_w = 100$ kg	None

[27] They established that by increasing the composition above 20% by weight of PHB the system becomes incompatible. The glass transition temperature (T_g) of PMMA was suppressed to an extent consistent with the solubility of PHB.

PVAc blends appear to be miscible over the blend range. Both Greco and Martuscelli [28] and Kumagai [29] have reported that PHB and PVAc were compatible and that their biodegradability fell off with increasing PVAc content [30]. Consequently PHB–PVAc blends exhibited a single glass transition and there was a depression of the equilibrium melting temperature of the PHB. Gassner and Owens [31] have studied other acetate systems—e.g. ethylene–vinyl acetate/Biopol blends and they identified two glass transitions and melting regions relating to the phase separated components. Mechanical testing showed that with over 70% Biopol the samples were stiff and relatively brittle. Zhang and Deng [32] also observed in PHB/hydroxyethylcellulose acetate blends that with a PHB content above 20%, the melting temperature of the PHB was independent of the blend composition, and the melting enthalpy was proportional to the amount of PHB present. The crystallisation of the PHB in the blends was reduced by the presence of the acetate component.

This paper considers the effect of PVAc in altering the crystallisation behaviour and morphology of PHB with the object of inhibiting embrittlement on storage.

2. Experimental

Poly(D-(−)3-hydroxybutyrate) (PHB) and copoly(D-(−)-3-hydroxybutyrate-*co*-8%-D-(−)-3-hydroxyvalerate) (CHB/HV) with added nucleating agent, were obtained as research samples from Zeneca Bioproducts, Billingham. We are grateful for the gift of these samples. Polyvinyl acetate (PVAc) was obtained from Sigma Aldrich Chemicals, UK. Polymer and copolymer characteristics are listed in Table 1.

Blends were prepared on a Schwabenthan heated twin roll mill, set to 180 and 190°C. The crepe produced was compression moulded into 2 mm thick plaques on a hydraulic press at 10 tonnes between Teflon sheets. The plaques were rapidly quenched in ice/water and stored under refrigeration at −5°C. These plaques were amorphous as measured by DSC and wide angle X-ray scattering.

A Perkin Elmer differential scanning calorimeter, DSC-2, interfaced to a PC-via an a/d converter, was used to characterise the thermal properties of the blends. Sub-ambient temperatures were achieved by liquid nitrogen cooling of the calorimeter block and its temperature maintained at 190 K. Blend samples in the form of 10–15 mg discs were cut from the moulded plaques, placed in aluminium pans and covered with an aluminium lid. The amorphous samples crystallised at room temperature and were made amorphous by heating the semi-crystalline samples to above their observed melting points, 470 K, and quenched in liquid nitrogen. These samples were placed in the calorimeter below 270 K. The temperature scale of the DSC was calibrated from the melting points of *n*-dodecane (263.6 K), zone-refined stearic acid (343.5 K), and 5 9s pure indium (429.8 K) and tin (505.06 K). The thermal response of the calorimeter was calibrated from the heat of fusion of indium, assumed to be 28.4 J g^{-1}. An empty aluminium pan was used as the reference in the calorimeter and the thermal lag was corrected by extrapolating to zero heating rate.

A Linkam, model TH600, hot stage was mounted on the X-Y stage of a Leitz Dialux-Pol polarised light microscope with a TV camera attachment, video recorder and video timer. A video of the development of the isothermal crystallisation was made and subsequently analysed using a Linkam video text overlay to measure the size of the spherulites. Specimens of thickness 20 μm were mounted on glass cover slips and placed in the furnace of the hot stage, the temperature of which was raised or lowered or held constant by a PR600 temperature controller.

3. Results and discussion

3.1. The glass transitions of the blends

The glass transition temperatures, T_gs, of the quenched amorphous blends were measured by DSC, from the step change in heat capacity using Richardson and Savill [33] method. The T_gs for PHB and PVAc were found to be 274 ± 1 and 313 ± 1 K, respectively. Both were in reasonable agreement with the generally accepted values for these polymers. Only one glass transition was observed for all the blends (Fig. 1) and the temperature at which this occurred varied with composition (Table 2) implying that the two

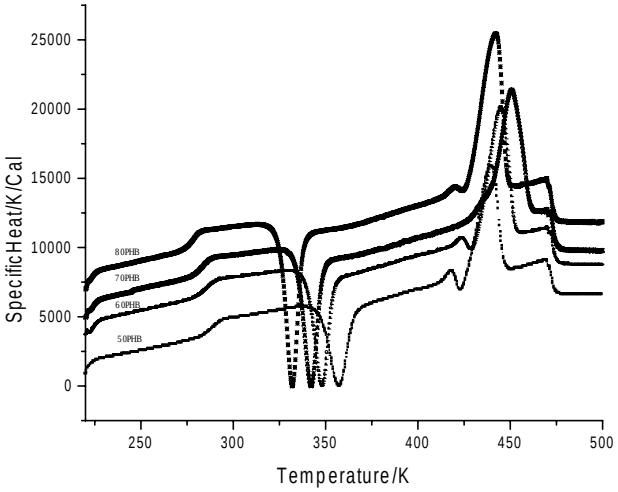

Fig. 1. DSC analysis of the blends showing the variation of T_g, T_c and T_m with composition.

components were miscible over the complete composition range studied.

The T_g dependence on composition exhibited a negative deviation from the linear change in T_g with composition, and could be fitted to the Gordon–Taylor equation [34] with an interaction parameter b of -1.00 ± 0.10, i.e.

$$b = T_g(W_1T_{g1} + W_2T_{g2})/W_1W_2(T_{g1} - T_{g2}) \quad (1)$$

where W_1 and W_2 are the weight fractions of PVAc and PHB, and T_{g1} and T_{g2} are their respective glass transition temperatures.

From the presence of a single glass transition temperature, it is clear that the blends are miscible over the complete range of compositions. This is due to specific interactions between the two homopolymers as indicated by the negative value of the interaction parameter b.

3.2. The crystallisation of the blends

The crystallisation kinetics of the blends were analysed by DSC using procedures adopted previously [35]. In a study of the high-temperature crystallisation, the blends were melted 10 K above the measured melting point, cooled at 180 K min^{-1} to the crystallisation temperature and held there until the crystallisation was complete, as indicated by the return of the calorimeter response to the baseline. The overall time dependence of the crystallisation (Fig. 2) was analysed using the Avrami equation, which relates the extent of crystallinity, X_t, to time, t,

$$1 - X_t = \exp[-Zt^n] \quad (2)$$

where Z is a composite rate constant incorporating both nucleation and growth and n the Avrami exponent is a constant characteristic of the crystallisation mechanism, Assuming

$$X_t = \int_0^t [dH/dt]\, dt \int_0^x [dH/dt]\, dt \quad (3)$$

the extent of crystallinity was determined as a function of time from the ratio of the areas under the curve, and the development of crystallinity analysed from a linear plot of $\log[-\ln\{1 - X_t\}]$ against $\log t$, for which the slope is n. An average value of Z was determined from the half life, $t_{1/2}$, since $Z = \ln 2/(t_{1/2})^n$.

For each crystallisation temperature and blend composition, the n values, the overall rate constant Z and the half life $t_{1/2}$, were separately measured and are shown in Table 3. The value of n for all the blends and PHB was about 2.5 ± 0.2 and did not appear to vary substantially either with composition or temperature. This value was consistent with the growth of predetermined spherulites with impurity rejection of PVAc from the growth fronts.

In crystallisations, close to the melting point of PHB (T_m) the phase transition is nucleation controlled and the crystallisation rate, as measured by the reciprocal of the half life, should increase with supercooling, i.e. $(T_m - T_c)$. This was observed for all the blends, as can be seen in Fig. 3, where the $\ln(t_{1/2})$ is plotted against the crystallisation temperature. However, the observed trend in rate with blend composition was completely unexpected in that the PVAc did appeared

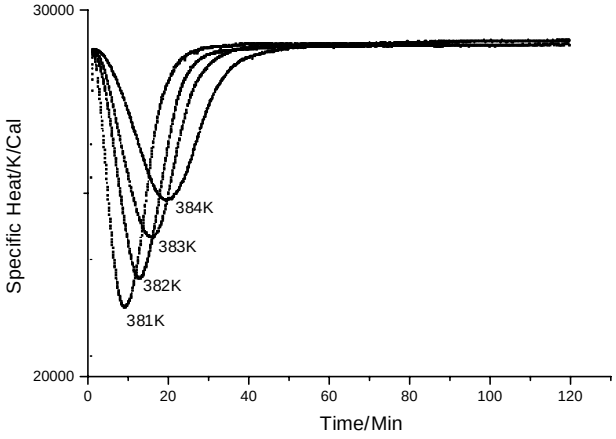

Fig. 2. DSC isothermal crystallisation.

Table 2
The glass transition temperature for PHB:PVAc blends

%PVAc	Calculated[a] T_g (K)	Observed T_g (K)
100	313 ± 1.0	313 ± 1.0
90	308 ± 1.0	300 ± 1.0
80	304 ± 1.0	293 ± 1.0
70	300 ± 1.0	292 ± 1.0
60	296 ± 1.0	287 ± 1.0
50	292 ± 1.0	285 ± 1.0
40	288 ± 1.0	280 ± 1.0
30	285 ± 1.0	279 ± 1.0
20	281 ± 1.0	275 ± 1.0
10	277 ± 1.0	274 ± 1.0
0	274 ± 1.0	274 ± 1.0

[a] From the Gordon–Taylor equation.

Table 3
Crystallisation rate constants for the bulk crystallisation of the blends—high-temperature crystallisation

Temperature (K)	Half life (min)	*n* Value (±0.2)	Rate constant *Z* (min^{-n})
(i) 0% PVAc			
381	8.6	2.3	5.41×10^{-3}
382	11.2	2.6	1.10×10^{-3}
383	13.9	2.8	4.61×10^{-4}
384	16.8	2.7	3.50×10^{-4}
385	26.6	2.5	2.10×10^{-4}
386	44.2	2.5	5.60×10^{-5}
(ii) 10% PVAc			
390	7.8	2.6	3.30×10^{-3}
392	12.6	2.6	1.10×10^{-3}
393	14.7	2.0	2.90×10^{-3}
394	18.1	2.2	2.70×10^{-3}
395	26.0	2.4	2.60×10^{-4}
397	27.3	2.2	4.20×10^{-4}
398	29.0	2.2	5.90×10^{-4}
399	32.5	2.2	2.80×10^{-4}
(iii) 20% PVAc			
380	6.40	2.5	7.00×10^{-3}
381	6.80	2.3	7.90×10^{-3}
383	7.50	2.2	7.50×10^{-3}
385	8.60	2.3	3.60×10^{-3}
388	11.80	2.1	2.10×10^{-3}
390	19.36	1.9	2.30×10^{-3}
391	19.75	2.3	2.30×10^{-3}
(iv) 30% PVAc			
380	5.70	2.5	8.90×10^{-3}
381	6.40	2.4	7.90×10^{-3}
382	7.00	2.2	9.60×10^{-3}
383	8.00	2.4	4.80×10^{-3}
384	8.50	2.5	3.40×10^{-3}
385	8.80	2.3	6.20×10^{-3}
386	9.50	2.6	1.90×10^{-3}
389	12.06	2.4	1.90×10^{-3}
(v) 40% PVAc			
389	6.0	2.7	5.90×10^{-3}
390	6.60	2.8	3.40×10^{-3}
391	6.70	1.9	1.90×10^{-2}
396	9.80	2.3	3.80×10^{-3}
398	10.90	2.1	4.70×10^{-3}
399	15.50	2.1	1.30×10^{-3}
(vi) 50% PVAc			
390	6.10	2.1	1.50×10^{-2}
391	6.70	2.2	9.70×10^{-3}
392	7.80	2.3	6.60×10^{-3}
394	8.70	2.5	3.30×10^{-3}
395	10.3	2.2	3.80×10^{-3}
396	11.27	2.1	4.80×10^{-3}
(vii) 60% PVAc			
395	5.10	2.4	1.30×10^{-2}
400	5.90	2.8	4.60×10^{-3}
401	6.80	2.9	2.50×10^{-3}
402	8.70	2.7	2.00×10^{-3}
403	9.3	2.8	1.70×10^{-3}

to be accelerating the crystallisation. The more PVAc was present the faster was the crystallisation rate at any temperature. This is inconsistent with either a lowering of the melting point of PHB by the addition of soluble PVAc or the presence of a non-crystalline component in the blends.

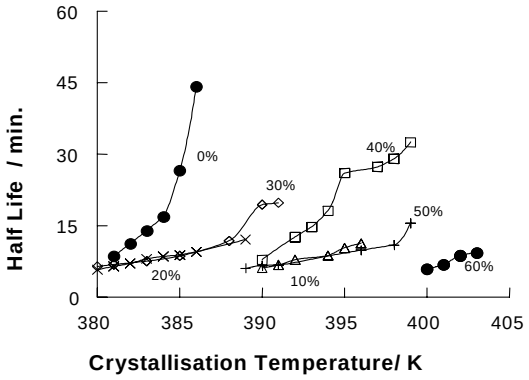

Fig. 3. Dependence of half lives on crystallisation temperature, T_c, close to the melting point.

Low-temperature crystallisations of the blends were also measured using the same procedure as before but by initially quenching the molten samples in liquid nitrogen, and raising the temperature at 180 K min^{-1} through the glass transition temperature to the crystallisation temperature. The isothermal-rate–time curves (Table 4) were analysed as described above for the higher temperature crystallisations.

Again for each crystallisation temperature and blend, the values of *n*, *Z*, and the half-life $t_{1/2}$, were determined and the values are listed in Table 4. No marked change in *n* value was observed with composition and it was similar to that observed at higher temperatures.

Close to the glass transition the rate of crystallisation increases with increasing temperature depending on the Williams–Landel–Ferry [36] relationship:

$$\ln(t_{1/2}) = \ln t_0 + (\Delta E/\mathrm{R})(T_c - T_g + 30) \quad (4)$$

where R is the gas constant, t_0 a constant and ΔE the activation energy for viscous flow. The measured activation energies for the various blends are listed in Table 5. The values were greater for the blends than for PHB but there was no marked trend with PVAc content in the blends.

Since crystallisation does not develop below the glass transition, allowance was made for the difference in the glass transition temperatures of the blends with composition, and $\ln(t_{1/2})$ was plotted against $(T_c - T_g)$ (Fig. 4). Despite this correction it was still apparent that the crystallisation was progressively inhibited by increasing amounts of PVAc and the value of $(T_c - T_g)$ at constant half life increased with PVAc composition.

There is clearly a conflict of evidence in that the presence of the PVAc both inhibits the crystallisation of the blends at low temperatures and accelerates it at temperatures close to the melting point. The similarity in the observed value of the Avrami exponent *n* in the two temperature regions is inconsistent with any overall change in crystallisation mechanism and rejection of PVAc from the crystalline

Table 4
Crystallisation rate constants for the bulk crystallisation of the blends—low-temperature crystallisation

Temperature (K)	Half life (min)	n Value (±0.2)	Rate constant Z (min^{-n})
(i) 0% PVAc			
298	17.2	2.6	4.10×10^{-4}
299	10.5	2.6	1.70×10^{-3}
300	8.10	2.6	2.80×10^{-3}
301	6.70	2.6	4.90×10^{-3}
302	6.00	2.3	1.70×10^{-2}
303	5.00	1.7	6.90×10^{-2}
(ii) 10% PVAc			
297	23.0	2.9	8.80×10^{-5}
298	14.7	2.6	5.70×10^{-4}
299	11.6	2.5	1.50×10^{-4}
300	8.00	2.2	7.80×10^{-3}
301	6.10	2.7	5.50×10^{-3}
303	17.2	2.8	7.70×10^{-3}
(iii) 20% PVAc			
307	17.9	2.3	1.00×10^{-3}
308	8.60	1.8	1.40×10^{-2}
309	7.90	2.1	1.70×10^{-2}
310	6.00	2.5	1.80×10^{-2}
311	5.10	1.8	3.50×10^{-2}
312	5.00	1.7	7.10×10^{-2}
(iv) 30% PVAc			
311	16.2	2.7	4.10×10^{-4}
312	14.4	2.6	6.70×10^{-4}
313	10.2	2.3	3.10×10^{-3}
314	9.10	2.4	3.20×10^{-3}
316	7.10	2.6	4.10×10^{-3}
(v) 40% PVAc			
321	8.60	2.9	1.50×10^{-3}
322	7.60	2.7	2.80×10^{-3}
323	7.00	3.0	2.00×10^{-3}
324	6.10	2.9	3.70×10^{-3}
325	5.30	2.9	5.80×10^{-3}
326	5.00	2.8	8.70×10^{-3}
(vi) 50% PVAc			
328	10.4	2.8	9.30×10^{-4}
329	8.50	2.5	4.70×10^{-3}
330	7.50	2.4	4.90×10^{-3}
331	6.40	2.6	5.60×10^{-3}
332	5.70	2.6	7.00×10^{-3}
333	5.00	2.7	1.00×10^{-3}
(vii) 60% PVAc			
336	8.30	2.9	2.14×10^{-3}
337	8.10	2.9	1.70×10^{-3}
338	6.50	2.3	9.30×10^{-3}
339	5.80	3.0	3.70×10^{-3}
341	5.10	2.4	2.50×10^{-2}

regions is more likely to be important at high rather than low crystallisation temperatures.

In order to check that PVAc did not co-crystallise with PHB by being incorporated into the crystalline regions, wide angle X-ray diffraction studies were carried out on the crystalline blends. The diffraction patterns of the blends were similar to one another and identical to that obtained from PHB (Fig. 5). There were no additional peaks present

Table 5
Activation energy for low-temperature crystallisation of the blends

PVAc content (%)	E (kJ mol^{-1})
0	6.1 ± 0.5
10	7.1 ± 0.5
20	6.9 ± 0.5
30	6.7 ± 0.5
50	6.8 ± 0.5
60	7.1 ± 0.5
Average	6.9 ± 0.6

Table 6
WAXS % crystallinity of the blends

Sample (% PHB content)	% Crystallinity	%-PHB crystallised	%-PHB in the amorphous phase
50	19	38	40
60	21	35	50
70	23	33	60
80	23	30	75
90	25	28	85
100	40	40	100

which increased in intensity with increasing amounts of PVAc but only an overall reduction in crystallinity clearly indicating that the crystalline phase was PHB only. The percentage crystallinities of the blends, measured from the ratio of the areas under the crystalline to amorphous scattering bands, were consistent with the amount of PHB present and a constant degree of crystallinity within the crystalline phase.. Bulk PHB was observed to be about 40% crystalline and the blends were less than this. Correcting for the reduced PHB content, the crystalline phases were about 30–40% of the total PHB available. Clearly some of the PHB was retained within the amorphous phase along with the PVAc (Table 6).

3.3. Hot stage microscopy of the blends

Analysis of the crystallisation rate by the Avrami equation determined a composite rate constant Z, which includes both growth rate g, and nucleation density. In order to elucidate the anomalous behaviour between high- and low-temperature crystallisation of the blends, the individual growth rates and nucleation characteristics were measured directly using polarised light hot stage microscopy.

At high temperatures, crystallisation was observed to develop from a small number of spherulites with characteristic Maltese cross and banded birefringence. Large several millimetres in diameter, developed on crystallising PHB from the melt, due to the very low nucleation density [39]. The radius of the spherulites increased linearly with time up to the point of impingement with adjacent spherulites. All

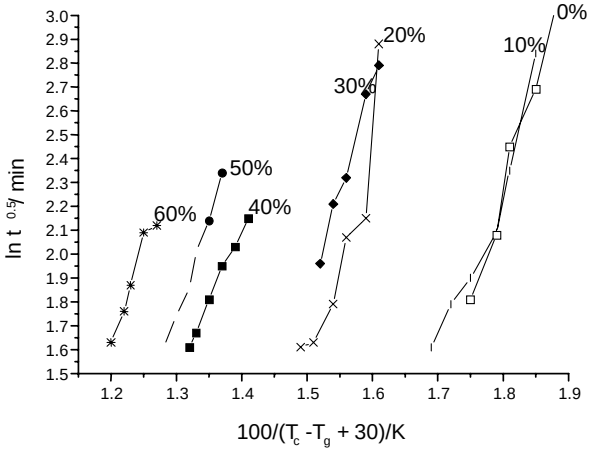

Fig. 4. Dependence of half life of crystallisation on superheating from T_g.

the blends crystallised in this manner except that the spherulitic texture became progressively coarser with more open texture and less well-defined boundaries between the spherulites and the melt with increasing PVAc content. This is consistent with crystallisation of the PHB as spherulites and rejection of the PVAc into the interlamellar regions. Nucleation of the spherulites was pre-determined as the number did not increase with time after an initial induction period of increasing numbers of nuclei.

There was no apparent induction time for the nucleation of the spherulites and the radius increased linearly with time in all the blends. The radial growth rate, $g = dr/dt$, where r is the spherulitic radius at time t, decreased with increasing crystallisation temperature and at the same temperature with increasing PVAc (Fig. 6) but crystallisation developed over the same high degree of supercooling, 75–110 K.

The exact opposite trend, however, was observed with nucleation density in that the number of spherulites observed increased substantially as more and more PVAc was adde. PHB is known to have a very low nucleation density and progressive additions of the PVAc was seen to be adding increasing amount of heterogeneous particles which act as crystallisation nuclei. As the levels of PVAc increased more nuclei are present in the blends and the bulk crystallisation rate increases. This is particularly so at high temperatures where the nucleation density is so low. At lower temperatures, close to T_g, the nucleation density is correspondingly higher and in the blends nucleation then becomes independent of PVAc content. The crystallisation rates then follows the expected trend with blend composition and the soluble PVAc retarded the crystallisation of PHB.

3.4. Melting studies on the blends

Soluble non-crystallisable impurities suppress the equilibrium melting points of polymers, T_m^0, and so depress the temperature range over which crystallisation can occur. The

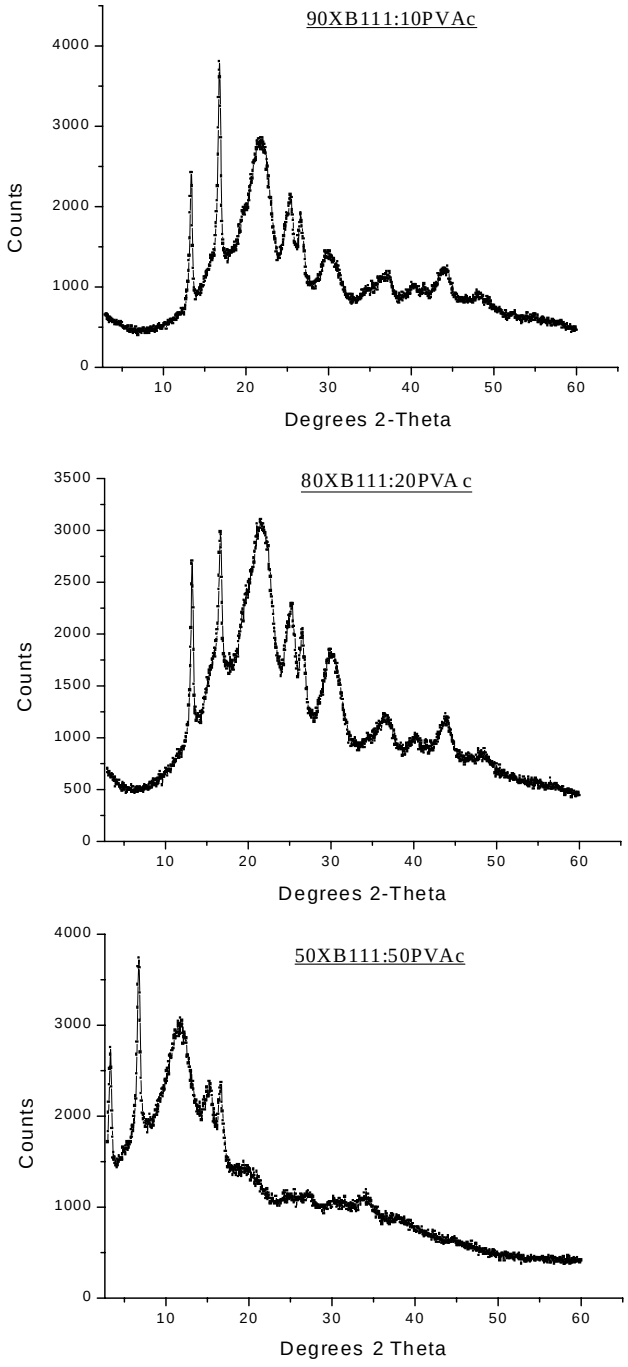

Fig. 5. Wide angle X-ray scattering of the blends.

equilibrium melting points of the blends, T_m^0, were determined using the Hoffman and Weeks [37] method from the dependence of the observed melting point T_m, on crystallisation temperature T_c, and by extrapolating to the equilibrium line of $T_m = T_c$ at T_m^0, since

$$T_m = (1 - 2/\beta)T_m^0 + T_c/2\beta \quad (5)$$

where $\beta = l_e\sigma/l\sigma_e$ and σ and σ_e are the energies of fold surface and l and l_e are the fold lengths during crystallisation

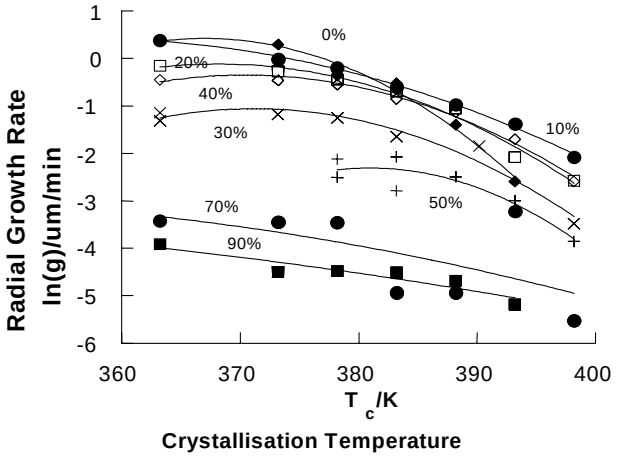

Fig. 6. Effect of blend composition on spherulite radial growth rate.

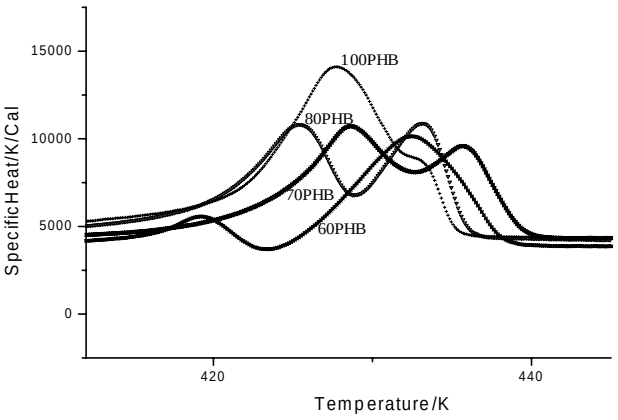

Fig. 7. Multiple melting in polymer blends.

and under equilibrium conditions. For equilibrium conditions to hold the slope of the line must be 0.5. Organ and Barham [38] applying this procedure showed that the T_m^0 obtained for PHB was low due to the thermal decomposition of PHB in the melt, but a value of 470 ± 2 K was determined.

Depending on the crystallisation temperature, PHB and the blends exhibited multiple melting endotherms (Fig. 7). This has been interpreted as being due to initial melting, re-crystallisation and subsequent melting of this material. The final melting endotherm does not relate to the crystallisation temperature, T_c. To overcome this problem a different procedure was adopted. The blends were crystallised at standard temperatures and subsequently annealed at higher temperatures for 60 min. It was first established that holding the PHB sample at these annealing temperatures up to 60 min did not lower the melting endotherms, so ensured that the T_m value observed was characteristic of the annealing temperature, T_a, and recrystallisation did not occur on melting. Plots of T_m against T_a were linear at the higher annealing temperatures and could be extrapolated with $\beta = 1$ to T_m^0. The values of $T_m^0(x)$ where x is the monomer mole fraction of PHB, listed in Table 7. These values were consistent with the polymer and not the monomer units lowering the melting point of PHB but the overall depression was too small to be measured by this method within the experimental error of ±2 K.

The temperature dependence of the radial growth rates was analysed by the Lauritzen–Hoffman [39] approach in order to determine the effect of the added PVAc in changing the free energy of the fold surface of the lamellae. The growth rate g, is

$$g = g_0 \exp[-\Delta E/\mathrm{R}(T_c - T_g + 30)] \exp[-K/(f\,T_c \Delta T)] \quad (6)$$

where g_0 is a constant, ΔE the activation energy associated with the glass forming process, ΔT the degree of supercooling from the equilibrium melting point, T_m^0, T_g is the glass transition temperature and K is a nucleation constant, and

$$f = 2T_c/(T_c + T_m^0) \quad (7)$$

Rearranging gives

$$\ln(g) + \frac{\Delta E}{\mathrm{R}(T_c - T_\infty)} = \ln(g_0) - \frac{K_g}{f\,T_c \Delta T} \quad (8)$$

It was assumed that the crystallisations were carried out in Regime III, so that,

$$K_g = 4b_0 \sigma \sigma_e T_m^0/(\Delta H_f)\mathrm{k} \quad (9)$$

where k is Boltzmann's constant and

$$\sigma = 0.1(a_0 b_0)^{1/2} \Delta H_f \quad (10)$$

Plots of $[\ln(g) + \Delta E/\mathrm{R}(T_c - T_g + 30]$ against $(T_c + T_m^0)T_m^0/2T_c^2(\Delta T)$ were linear with slopes $(4b_0\sigma\sigma_e/\Delta H_f\mathrm{k})$. Although the observed linear dependencies were displaced relative to one another they had similar slopes (Fig. 8) and accordingly very similar values for the free.

The lateral position of the lines depended on $\ln(g_0)$ and in turn the value chosen for E, the activation energy of viscous flow and all the lines could be superimposed by suitable choice of the activation energy. It is apparent that the difference in temperature dependence of the growth rates mainly arose from changes in the viscosity of the melt with composition, and not to any change in surface free energy or crystallisation mechanism, which is clearly that of predetermined nucleation of spherulites.

4. Discussion

The binary phase diagram for the blend system PHB/PVAc is shown in Fig. 9. Blends quenched from above the equilibrium melting points are amorphous and exhibit a single glass transition whose temperature increase progressively with PVAc content. The polymers are clearly soluble at all compositions over the temperature range

Table 7
The variation of the equilibrium melting point with blend composition

PVAc (%)	T_m^0 (K)	Slope (K_{ll}/K^{-1})	ln (g_0)	Nucleation density[a] (no. mm^{-3})
0	474 ± 2	1280	10.23	1.4
10	475 ± 2	1030	7.38	280
20	475 ± 2	1160	9.90	80
30	474 ± 2	1120	8.60	20
50	469 ± 2	1205	9.00	30

[a] Nucleation density at 363 K.

studied. Heating to temperatures above the glass transition is followed by crystallisation of PHB from the melt and the rate of the conversion varied with temperature and composition. The equilibrium melting point of the PHB at low PVAc content was independent of composition of the blend and within the experimental error identical to that of PHB. This behaviour was consistent with the PVAc polymer rather than the monomer units acting as impurities and lower the melting point. WAXS studies showed that PHB alone crystallised and the overall degree of crystallinity of the PHB was independent of composition. Microscopic examination of the spherulites which developed during crystallisation showed that there was no change in mechanism with increasing PVAc content but an increasing coarsening of the spherulites with PVAc being rejected from the crystalline regions.

The texture and shape of the spherulites are markedly affected by blend composition, since on increasing PVAc content the surface of the spherulite becomes rougher and granular in appearance with a distortion from the spherical shape and the development of less well-defined spherulite boundaries. The texture and shape of the spherulite is consistent with impurity rejection from the growing lamellae.

The differences in the observed rates of bulk crystallisation of the blends at low temperatures is consistent with the increase in T_g of the blends and could be accounted for partially by the degree of superheating from the glass

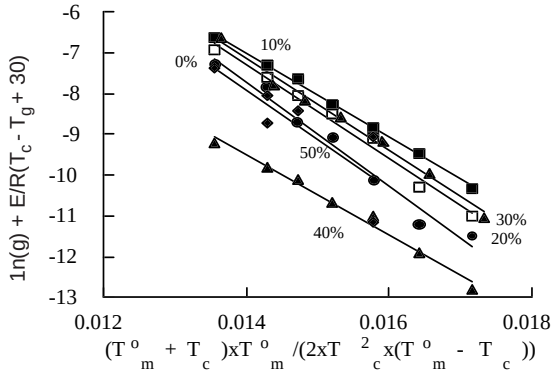

Fig. 8. Temperature dependence of radial growth rates.

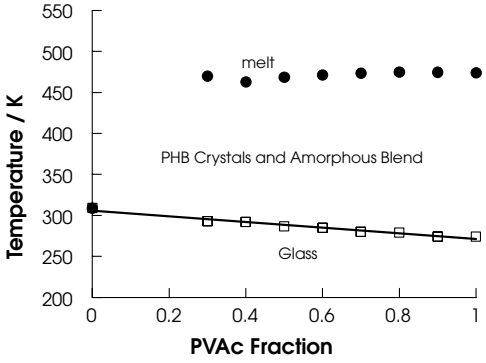

Fig. 9. Binary phase diagram—PHB/PVAc blends.

transition, and the activation energy of melt flow. This was not the case, however, with the high-temperature crystallisation where the observed half lives increased with PVAc content rather than decrease as expected. The spherulitic growth rates, however, did decrease with decreasing degree of supercooling and with added PVAc content. We attribute this anomaly to increasing nucleation of the crystallisation of PHB in the blends and to the extremely low levels of nuclei present in the natural polymer.

From the Avrami equation for the isothermal crystallisation of predetermined spheres from the bulk at the half life, $t_{1/2}$,

$$N = \ln(2)/(4/3\pi g^3 t_{1/2}^3) \quad (11)$$

where N is the nucleation density.

Combining the growth rates, and half-lives the nucleation density at a constant degree of supercooling was determined for the blends. This is listed in Table 7. It can clearly be seen that the nucleation density increases but not in line with the amount of added PVAc in the blends. Blending alone clearly increases the nucleation density and this was further tested by blending PVAc with the copoly(D-(−)-3-hydroxybutyrate-*co*-8%-3-D-(−)-3-hydroxyvalerate (XB111) containing 1% BN as a nucleating agent. There is sufficient nuclei in this seeded sample to swamp any further addition on blending. Measurement by DSC of the bulk crystallisation showed that the crystallisation half-lives decreased with PVAc content (Fig. 10) in line with PVAC retarding the crystallisation. The effect was not marked.

5. Conclusions

The anomalous crystallisation behaviour of PHB blends has been attributed to an increase in the nucleation density on blending either due to nucleating impurities added in the blending process. The low nucleation density, which skews the crystallisation-rate–temperature dependence of PHB

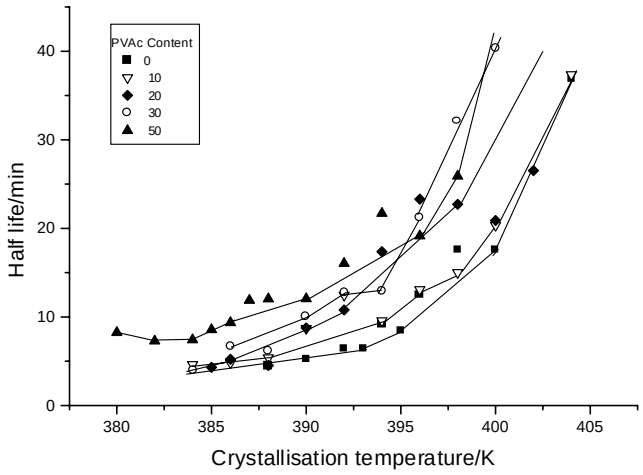

Fig. 10. The effect of PVAc on the crystallisation half-lives of the BN seeded copolymer.

towards low temperatures, makes it particularly sensitive to these chance impurities.

The addition of the PVAc to PHB reduces the rate of crystallisation close to the glass transition, and accordingly would be expected to reduce the dependence of the blends, compared with the homopolymer, to embrittlement on storage at room temperature. The PVAc blends excluded from the crystallisation will act as rubber particles and so toughen the resulting composites.

References

[1] Zeneca Ltd, Biopol Resin Natures Plastic, copyright Zeneca Ltd, 1993.
[2] Williams S, Peoples O. Chem Br 1997;33(12):29.
[3] Grace WR, Co., USA patent, 3 (1956) 225, 766.
[4] Holmes PA. Phys Tech 1985;16:32.
[5] Union Carbide Co., US Patent, 4 (1984) 372, 311.
[6] Akhtar S. Polymer 1992;33(1):117.
[7] Schmitt E. US Patent, Apr 8, 3 (1975) 875, 937.
[8] Marchessault RH, Alper J. Biopolymers 1963;1:545–56.
[9] Juni K, Nakano M. J Controlled Release 1986;4:125.
[10] Hanggi VJ. Novel biodegradable microbial polymerisation. NATO ASI Series 1990;186:65.
[11] Holland SJ, Tighe BJ. Biomaterials 1987;July 8:289–95.
[12] Doi Y. Microbial polyesters, New York: VCH Publishers, 1990.
[13] Barham PJ, Keller A. J Polym Sci 1986;24:69.
[14] Scandola M, Ceccorulli G, Pizzoli M. Makromol Chem Rapid Commun 1989;10:47.
[15] de Koning GJM, Lemstra PJ. Polymer 1993;34:4089.
[16] de Koning GJM, Lemstra PJ. Polymer 1992;33:3295.
[17] de Koning GJM, Peeters M, Scheeren AHC, Reynaers H, Lemstra PJ. Polymer 1994;35:4598.
[18] Hay JN, Harris A, Biddlestone F, Hammond T. Polym Int 1996;39:221–9.
[19] Holmes PA. In: Bassett DC, editor. Developments in crystalline polymers—2, London: Elsevier, 1988.
[20] Ray AR, Sharma R. J Macromol Sci—Rev Macromol Phys 1995;C35(2):327.
[21] Martuscelli E, Avella M. Polymer 1988;29(10):1731.
[22] Martuscelli E, Avella M, Greco P. Polymer 1991;32(9):1647.
[23] Holland SJ, Tighe BJ, Yasmin M, Jolly AM. Biomaterials 1989;10:400.
[24] Holland SJ, Tighe BJ, Yasmin M. Biomaterials 1989;10:400.
[25] Reeve MS, McCarthy SP, Gross RA. Macromolecules 1993;26:888.
[26] Scandola M, Ceccorulli G, Pizzoli M, Lotti N. Polymer 1993;34(23):4935.
[27] Yoon JS, Choi CS, Maing SJ, Hyoung JC, Lee HS, Choi SJ. Eur Polym J 1993;29(10):1359.
[28] Martuscelli E, Greco P. Polymer 1989;30:1475.
[29] Kumagai K. Polym Degn Stability 1992;36:241.
[30] Kumagai K. Doi. Sumitomo Kinzoku 1992;44(5):156.
[31] Owens AJ. Gassner. Polymer 1992;33(12):2508.
[32] Zhang L, Deng X, Zhao S, Huang Z. Polymer 1997;38(24):6001.
[33] Richardson MJ, Savill NG. Polymer 1975;16:753.
[34] Gordon M, Taylor J. J Appl Chem 1952;2:493.
[35] Booth A, Hay JN. Polymer 1969;10:95.
[36] Keith HD, Padden FJ. J Appl Phys 1964;35(4):1270.
[37] Hoffman JD, Weeks JJ. J Res Natl Bur Stand 1962;66A:13.
[38] Barham PJ, Organ SJ. J. Mater Sci 1991;26:1368.
[39] Hoffman JD, Frolen LJ, Ross GS, Lauritzen Jr JI, J J. J Res Natl Bur Stand 1975;79A(6):671.